13.4 % Efficiency from All-Small-Molecule Organic Solar Cells Based on a Crystalline Donor with Chlorine and Trialkylsilyl Substitutions

Very Important Paper

13.4% Efficiency from All-Small-Molecule Organic Solar Cells Based on a Crystalline Donor with Chlorine and Trialkylsilyl Substitutions

Wenyan Su[+],[a, b] Yang Wang[+],[c] Zhihong Yin[+],[c] Qunping Fan,*[b] Xia Guo,[c] Liyang Yu,*[d] Yuxiang Li,[e] Lintao Hou,*[a] Maojie Zhang,*[c] Qiang Peng,[d] Yongfang Li,[c] and Ergang Wang*[b, f]

How to simultaneously achieve both high open-circuit voltage (V_{oc}) and high short-circuit current density (J_{sc}) is a big challenge for realising high power conversion efficiency (PCE) in all-small-molecule organic solar cells (all-SM OSCs). Herein, a novel small molecule (SM)-donor, namely FYSM–SiCl, with trialkylsilyl and chlorine substitutions was designed and synthesized. Compared to the original SM-donor FYSM–H, FYSM–Si with trialkylsilyl substitution showed a decreased crystallinity and lower highest occupied molecular orbital (HOMO) level, while FYSM–SiCl had an improved crystallinity, more ordered packing arrangement, significantly lower HOMO level, and predominant "face-on" orientation. Matched with a SM-acceptor Y6, the FYSM–SiCl-based all-SM OSCs exhibited both high V_{oc} of 0.85 V and high J_{sc} of 23.7 mA cm^{-2}, which is rare for all-SM OSCs and could be attributed to the low HOMO level of FYSM–SiCl donor and the delicate balance between high crystallinity and suitable blend morphology. As a result, FYSM–SiCl achieved a high PCE of 13.4% in all-SM OSCs, which was much higher than those of the FYSM–H- (10.9%) and FYSM–Si-based devices (12.2%). This work demonstrated a promising method for the design of efficient SM-donors by a side-chain engineering strategy via the introduction of trialkylsilyl and chlorine substitutions.

Introduction

Organic solar cells (OSCs) have been considered as a promising candidate in the next-generation photovoltaic technologies due to their advantages of low cost, light weight, and semi-transparency and flexibility for the applications in building-integrated photovoltaics and wearable power generators.[1–3] Recently, with the rapid development of high-performance non-fullerene acceptors, especially ITIC (2,2′-[[6,6,12,12-tetrakis-(4-hexylphenyl)-6,12-dihydrodithieno[2,3-*d*:2′,3′-*d*′]-*s*-indaceno-[1,2-*b*:5,6-*b*′]dithiophene-2,8-diyl]bis[methylidyne(3-oxo-1*H*-indene-2,1(3*H*)-diylidene)]]bispropanedinitrile)[4] and Y6 (2,2′-((2*Z*,2′*Z*)-((12,13-bis(2-ethylhexyl)-3,9-diundecyl-12,13-dihydro-[1,2,5]thiadiazolo[3,4-*e*]thieno[2′′,3′′:4′,5′]thieno[2′,3′:4,5]pyrrolo-[3,2-*g*]thieno[2′,3′:4,5]thieno[3,2-*b*]indole-2,10-diyl)bis-(methanylylidene))bis(5,6-difluoro-3-oxo-2,3-dihydro-1*H*-indene-2,1-diylidene))dimalononitrile),[5] OSCs have achieved great progress in photovoltaic performance with power conversion efficiencies (PCEs) over 17%.[6–10] However, all the state-of-the-art OSCs have to employ polymer donors, even though the

[a] Dr. W. Su,[+] Prof. L. Hou
Guangzhou Key Laboratory of Vacuum Coating Technologies and New Energy Materials
Siyuan Laboratory, Department of Physics
Jinan University
Guangzhou 510632 (P. R. China)
E-mail: thlt@jnu.edu.cn
[b] Dr. W. Su,[+] Dr. Q. Fan, Prof. E. Wang
Department of Chemistry and Chemical Engineering
Chalmers University of Technology
Göteborg, 412 96 (Sweden)
E-mail: fanqp06@126.com
ergang@chalmers.se
[c] Y. Wang,[+] Z. Yin,[+] Prof. X. Guo, Prof. M. Zhang, Prof. Y. Li
Laboratory of Advanced Optoelectronic Materials, College of Chemistry
Chemical Engineering and Materials Science
Soochow University
Suzhou 215123 (P. R. China)
E-mail: mjzhang@suda.edu.cn
[d] Dr. L. Yu, Prof. Q. Peng
School of Chemical Engineering, and State Key Laboratory of Polymer Materials Engineering
Sichuan University
Chengdu 610065 (P. R. China)
E-mail: liyangyu@scu.edu.cn
[e] Dr. Y. Li
School of Materials Science and Engineering
Xi'an University of Science and Technology
Xi'an 710054 (P. R. China)
[f] Prof. E. Wang
School of Materials Science and Engineering
Zhengzhou University
Zhengzhou 450001 (P. R. China)
[+] These authors contributed equally to this work.

Supporting information for this article is available on the WWW under https://doi.org/10.1002/cssc.202100860

This publication is part of a collection of invited contributions focusing on "Advanced Organic Solar Cells". Please visit chemsuschem.org/collections to view all contributions.

polymers typically suffer from batch-to-batch variations in molecular weights and purity, which often leads to poor reproducibility in their photovoltaic performance in OSCs based on different batches of the "same" polymers.

Unlike polymeric materials, small molecular materials have several distinct advantages, such as easy purification, well-defined molecular structure, and excellent batch-to-batch replicability, which makes them priority candidates for commercialization and highlights the prospect of all-small-molecule (all-SM) OSCs.[11–13] However, all-SM OSCs used to have a low open-circuit voltage (V_{oc}) and/or short-circuit current density (J_{sc}) mainly due to the unmatched molecular energy levels and/or unsuitable blend morphology of SM-donor/SM-acceptor pair. As a result, the PCEs of all-SM OSCs lag far behind that of the OSCs based on polymer donors. Recently, a variety of molecular modification strategies,[14–17] especially the side chain engineering,[18–21] have been applied in the design of high-performance SM-donors for boosting the PCEs of all-SM OSCs. For example, by replacing a hexyl chain with a chlorine (Cl) atom on thienyl benzodithiophene (BDT) of the original SM-donor BTR (2,6-(5′′-yl-3′,3′′-dihexyl-[2,2′:5′,2′′-terthiophene]-5-(3-hexyl-5-methylene-2-thioxothiazolidin-4-one))-4,8-bis(5-(2-ethylhexyl-3-hexyl)thiophen-2-yl)benzo[1,2-*b*:4,5-*b*′]dithiophene), Lu and co-workers developed a SM-donor BTR-Cl[18a] with a deep-shifted highest occupied molecular orbital (HOMO) level, more ordered molecular packing, and improved crystallinity due to the large electronegativity of Cl atom, reduced dihedral angle between thienyl and BDT, and improved intermolecular interaction. Matching with Y6, an impressive PCE of 13.6% is achieved in the all-SM OSCs. Li and co-workers and Ge and co-workers introduced fluorine atom into thienyl BDT and thus synthesized SM-donors SM1-F[19a] and BTCE-2F[19b] with a deep-shifted HOMO level, modulated crystallinity, and optimized morphology in the blend active layers. In the Y6-based all-SM OSCs, they achieved PCEs over 13%. Janssen and co-workers developed a SM-donor H31 (2,6-(5′′-yl-3′,3′′-dihexyl-[2,2′:5′,2′′-terthiophene]-5-(2-ethylhexyl 2-cyano-3-acrylate))-4,8-bis(5-(2-ethylhexyl)thiophen-2-yl)benzo[1,2-*b*:4,5-*b*′]dithiophene) with a deep HOMO level by attaching trialkylsilyl to thienyl BDT.[20] Paired with Y6, the all-SM OSCs without electron transport layer (ETL) offered a PCE exceeding 13% and delivered a superior shelf lifetime compared to the reference devices with a ETL of PDINO. Recently, Hou and co-workers provided a simple and effective strategy that introduces two-dimensional (2D) phenyl-substitution into BDT core, to enhance the crystallinity of SM-donor and synergistically optimize the morphology of the all-SM blend.[21a] Moreover, the reported SM-donor B1 (2,6-(5′′-yl-3′,3′′-dihexyl-[2,2′:5′,2′′-terthiophene]-5-(3-hexyl-5-methylene-2-thioxothiazolidin-4-one))-4,8-bis((4-(2-ethylhexylthio)phenyl)-1-yl)benzo[1,2-*b*:4,5-*b*′]dithiophene) achieved an outstanding PCE of 15.3% in the all-SM devices, a large step forward in the all-SM OSCs field. However, although all-SM OSCs have made considerable progress, their PCEs are still lower than the polymer-based OSCs, which is mainly due to the lack of high-performance SM-donors and the difficulty to achieve both high V_{oc} and high J_{sc} in the all-SM OSCs.

Our previous work shows that the introduction of trialkylsilyl and/or chlorine into thienyl BDT unit of polymer donors can significantly reduce HOMO level, increase extinction coefficient, improve hole mobility, as well as modulate blend morphology simultaneously.[22] Inspired by the successes of the above SM-donors and our previous work, herein, we developed three SM-donors namely FYSM–H, FYSM–Si, and FYSM–SiCl, by attaching alkyl, trialkylsilyl, and both trialkylsilyl and Cl atom as substituents to thienyl BDT core, respectively. These SM-donors, from the original FYSM–H to FYSM–Si, and then FYSM–SiCl, show the gradually deep-shifted HOMO levels and increased hole mobilities. Compared to FYSM–H film, FYSM–SiCl film displays a reversed orientation from "edge-on" to "face-on". Moreover, the introduction of trialkylsilyl and Cl atom on thienyl BDT core modulates molecular crystallinity of SM-donors and thus optimizes their blend morphologies. As a result, compared to the FYSM–H:Y6-based all-SM OSCs (PCE = 10.9%, V_{oc} = 0.81 V, and J_{sc} = 22.2 mA cm^{-2}), the FYSM–SiCl:Y6-based ones achieved a much higher PCE of 13.4% benefitting from both higher V_{oc} of 0.85 V and higher J_{sc} of 23.7 mA cm^{-2}, while the FYSM–Si:Y6-based ones obtained a moderate PCE of 12.2% (V_{oc} = 0.82 V and J_{sc} = 22.4 mA cm^{-2}).

Results and Discussion

The synthetic routes and chemical structures of the three SM-donors are shown in Scheme 1 and Figure 1a, respectively, and the detailed synthesis processes are summarized in the Supporting Information. As displayed in Figure S1, in the thermogravimetric analysis (TGA) measurements, all three SM-donors have excellent thermal stability with a high decomposition temperature of approximately 380 °C at 5% weight loss.

The normalized UV/Vis absorption spectra of the four active layer materials in neat films are shown in Figure 1b. With the introduction of trialkylsilyl and Cl atom onto the thienyl BDT core, the three SM-donors FYSM–H, FYSM–Si, and FYSM–SiCl show similar but slightly blue-shifted absorption spectra in turn, which is mainly due to the increased steric hindrance effect of trialkylsilyl and Cl atom substitutions, as observed in previous work.[22a] The absorption onsets of the three SM-donors are located at 723, 700, and 681 nm, respectively, with the corresponding optical bandgaps (E_g^{opt}) of 1.72, 1.77, and 1.82 eV, which is complementary to the absorption of SM-acceptor Y6 with a E_g^{opt} of 1.34 eV. Moreover, as shown in Figure S2, the blend films show gradually increased absorbance from FYSM–H:Y6 to FYSM–Si:Y6 and FYSM–SiCl:Y6, suggesting that the FYSM–SiCl:Y6 pair can capture more photons for achieving higher J_{sc} in the resulting OSCs. Electrochemical cyclic voltammetry (CV) measurements were carried out to estimate energy levels of the three SM-donors, as shown in Figure 1c. According to the onsets of oxidation and reduction potentials (E_{ox} and E_{red}) of the three SM-donors and the equations of $E_{HOMO} = -(E_{ox} + 4.71)$ eV and $E_{LUMO} = -(E_{red} + 4.71)$ eV, the HOMO and lowest unoccupied molecular orbital (LUMO) levels are calculated as −5.23 and −3.59 eV for FYSM–H, −5.29 and

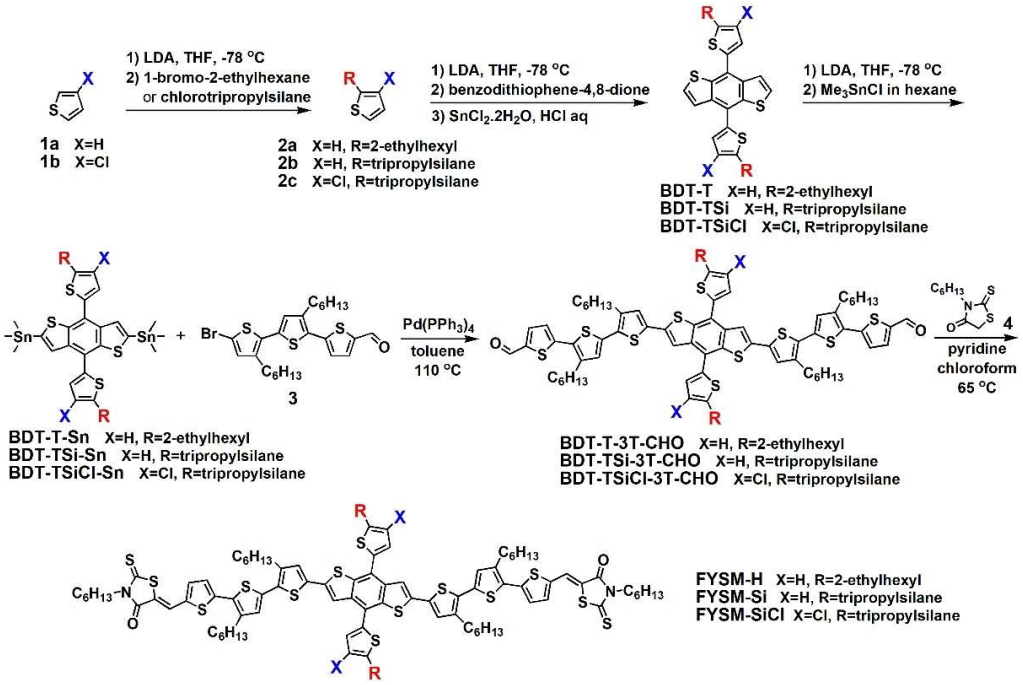

Scheme 1. Synthetic routes of three SM-donors of FYSM–H, FYSM–Si, and FYSM–SiCl.

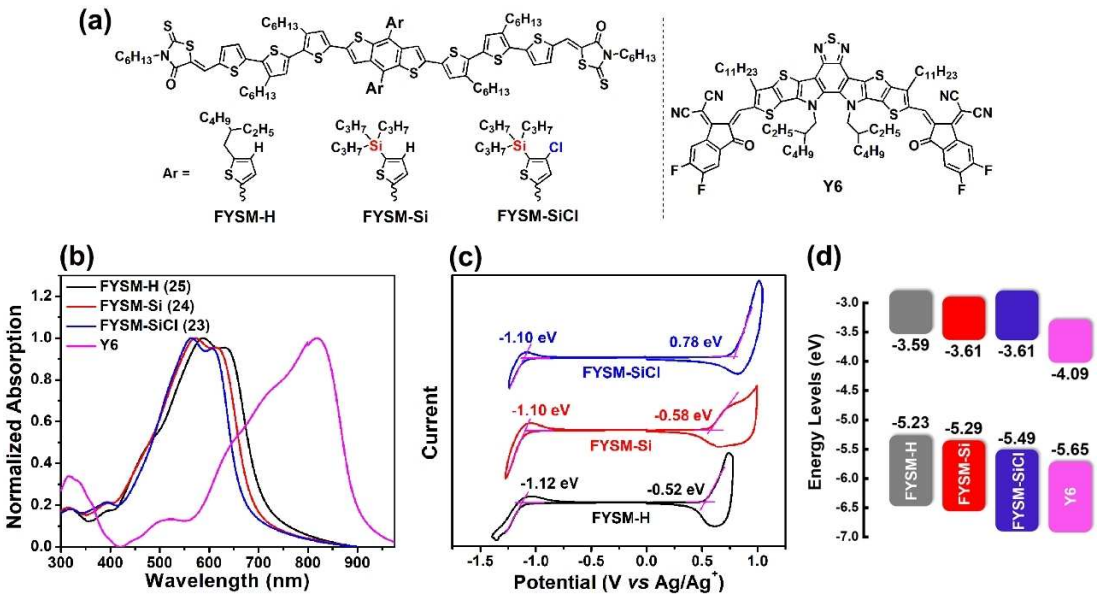

Figure 1. (a) Molecular structures of active layer materials and (b) the corresponding normalized absorption spectra. (c) Cyclic voltammograms of three SM-donors. (d) Energy level diagrams of active layer materials in neat films.

−3.61 eV for FYSM–Si, and −5.49 and −3.61 eV for FYSM–SiCl (Figure 1d), respectively. The above result indicates that, with the introduction of trialkylsilyl and Cl atom onto the thienyl BDT core, the SM-donors exhibit sequentially deep-shifted HOMO levels because of the σ* (Si)–π* (C) bond interaction from alkylsilyl substituent and the strong electronegativity from Cl atom substituent,[20,22a] which is in favor of a higher V_{oc} in the FYSM–SiCl-based all-SM OSC devices.

To probe the crystallinity of the three SM-donors, differential scanning calorimetry (DSC) measurements were performed. As shown in Figure 2a, among the three SM-donors, FYSM–H has the highest melting temperature (T_m) of 218 °C and a clear and sharp crystallization peak at 200 °C. Compared to FYSM–H, trialkylsilyl-substituted FYSM–Si shows two obviously weakened melting peaks at lower T_m of 162 and 183 °C (Figure 2b), and three much lower crystallization peaks at 134,

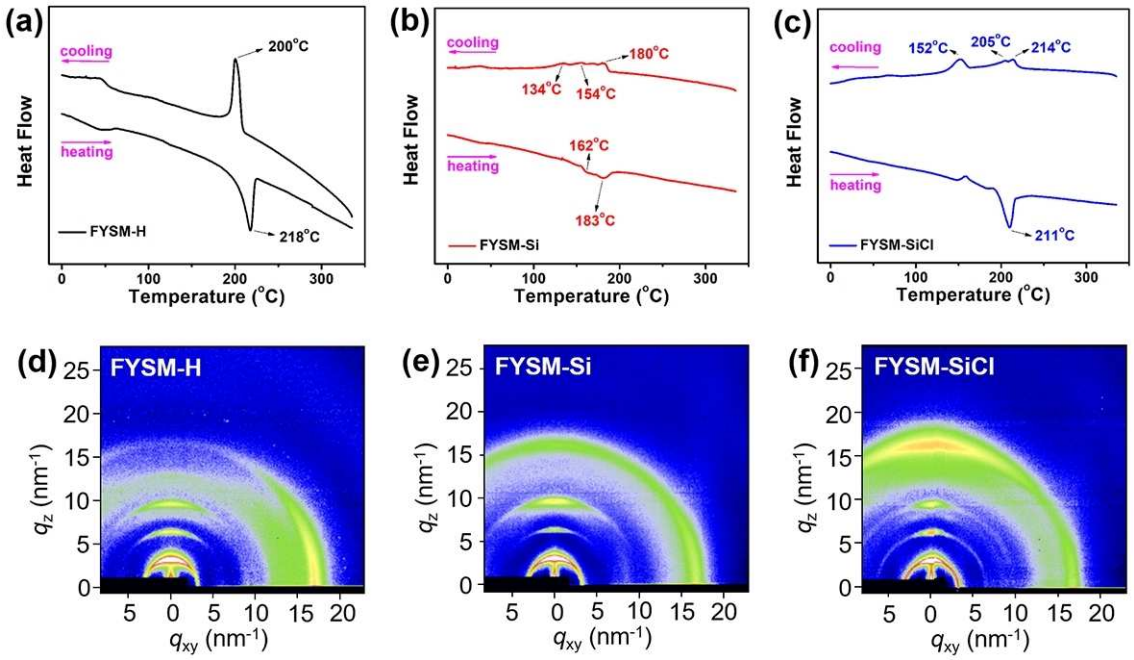

Figure 2. DSC curves and 2D GIWAXS profiles: (a,d) FYSM–H, (b,e) FYSM–Si, and (c,f) FYSM–SiCl.

154, and 180 °C. With the combined trialkylsilyl and Cl atom substitutions, FYSM–SiCl has a melting peak comparable to FYSM–H and much sharper than FYSM–Si (Figure 2c). Moreover, FYSM–SiCl displays two obvious and one weak crystallization peaks in a wide range of 152–214 °C, indicating relatively strong crystallinity with crystals formed at different temperatures. As shown in Figure 2d–f of the grazing incidence wide-angle X-ray scattering (GIWAXS) measurements, all three SM-donors in neat films have obvious multiple diffraction peaks of (100), (200), and (300) in the out-of-plane (OOP) direction, suggesting a highly ordered lamellar stacking and good crystallinity. Unlike the FYSM–H film with an "edge-on" dominant orientation as evidenced by a strong π–π stacking in the in-plane (IP) direction, the FYSM–Si film shows a mixed orientation of "edge-on" and "face-on" as evidenced by a diffuse circular π–π stacking diffraction, while FYSM–SiCl film has a "face-on" dominant orientation as evidenced by a strong π–π stacking in the OOP direction, indicating that the introduction of both trialkylsilyl and Cl atom substitutions can effectively reverse molecular orientation from "edge-on" to "face-on" in this case. The "face-on" dominant orientation of SM-donors is beneficial to the charge transport of the related OSCs. Hole mobilities (μ_h) of the three SM-donors were investigated by space-charge-limited current (SCLC) method. As shown in Figure S3 and Table S1, with the introduction of trialkylsilyl and Cl atom, SM-donors in the hole-only devices exhibit similar but slightly increased μ_h from 3.39×10^{-4} cm^2 V^{-1} s^{-1} for FYSM–H to 4.04×10^{-4} cm^2 V^{-1} s^{-1} for FYSM–Si and then 4.78×10^{-4} cm^2 V^{-1} s^{-1} for FYSM–SiCl.

The all-SM OSCs with a device structure of ITO/PEDOT:PSS/SM-donor:Y6/PFN–Br/Ag were fabricated to probe the effects of trialkylsilyl and Cl atom substitutions on photovoltaic performance of SM-donors. Considering their similar chemical structures, the all-SM OSCs based on the three SM-donors were fabricated using the same optimized processing conditions with Y6 as acceptor, in which the active layers with a similar thickness of approximately 90 nm were spin-coated from a chloroform solution (22 mg mL^{-1} in total solid, dissolved 4 h under 50 °C) of SM-donor:Y6 (*w*/*w*, 1:1) and then were treated by solvent vapour annealing (30 μL chloroform) for 60 s and thermal annealing for 10 min at 100 °C in turn. As shown in Figure 3a with the current density-voltage (*J*-*V*) curves and Table 1, from FYSM–H to FYSM–Si and then to FYSM–SiCl, the related devices achieved a gradually increased V_{oc} from 0.81 to 0.85 V, which is consistent with their down-shifted HOMO levels. Compared to the FYSM–H:Y6-based devices with a PCE of 10.9%, V_{oc} of 0.81 V, J_{sc} of 22.2 mA cm^{-2}, and fill factor (FF) of 60.8%, the FYSM–Si:Y6-based ones show a slightly increased V_{oc} of 0.82 V and J_{sc} of 22.4 mA cm^{-2} and an obviously improved FF

Table 1. Photovoltaic data of the Y6-based all-SM OSCs with different SM-donors.

Active layer	V_{oc}[a] [V]	J_{sc}[a] [mA cm^{-2}]	Calc. J_{sc}[b] [mA cm^{-2}]	FF[a] [%]	PCE[a] [%]
FYSM–H:Y6	0.81 (0.80)	22.2 (22.0)	21.4	60.8 (59.4)	10.9 (10.6)
FYSM–Si:Y6	0.82 (0.81)	22.4 (22.1)	22.0	66.6 (65.5)	12.2 (11.9)
FYSM–SiCl:Y6	0.85 (0.84)	23.7 (23.5)	22.5	66.8 (66.0)	13.4 (13.2)

[a] The average photovoltaic parameters in parenthesis were calculated from 10 independent devices. [b] The integral J_{sc} values in parenthesis were calculated from EQE curves, and the errors between integral J_{sc} from EQE and measured J_{sc} from *J*-*V* are within 5%.

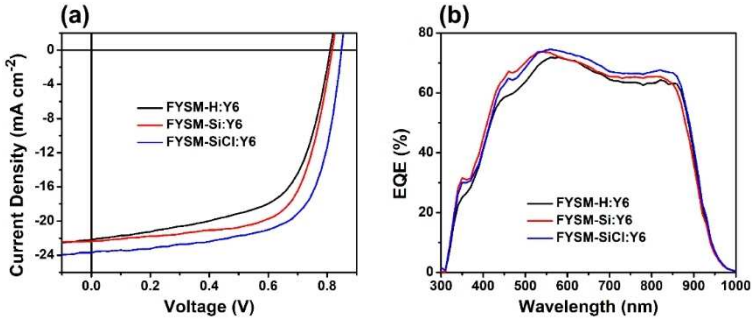

Figure 3. Photovoltaic performance of the Y6-based all-SM OSCs with different SM-donors: (a) *J-V* plots and (b) corresponding EQE curves.

of 66.6%, resulting in a moderate PCE of 12.2%. With the additional introduction of Cl atom, FYSM–SiCl achieved a further increased V_{oc} of 0.85 V and J_{sc} of 23.7 mA cm^{-2} and a similar FF of 66.8% in the devices, which boosts its PCE to 13.4%. The above result indicates that the introduction of both trialkylsilyl and Cl atom substitutions onto the SM-donors can synergistically improves V_{oc} and J_{sc} and thus boosts PCE of their all-SM OSCs.

External quantum efficiency (EQE) measurements were performed to probe the photon collection and verify J_{sc} values of the all-SM OSCs, as shown in Figure 3b. All devices show efficient photon collection, while the FYSM–SiCl:Y6-based all-SM OSC has higher EQE response in a wide range of 550–850 nm. The FYSM–SiCl-based device has a higher integrated J_{sc} of 22.5 mA cm^{-2} as calculated from the EQE curve compared to the devices based on FYSM–H (21.4 mA cm^{-2}) and FYSM–Si (22.0 mA cm^{-2}), which is consistent with the results from *J-V* measurements.

The exciton dissociation probabilities *P*(*E*,*T*) of the all-SM OSCs were evaluated by plotting the effective voltage (V_{eff}) versus the photocurrent (J_{ph}).[23,24] As shown in Figure 4a, compared to the FYSM–H:Y6-based device with a *P*(*E*,*T*) of 70.7% under the maximal power output condition, the devices based on FYSM–Si:Y6 and FYSM–SiCl:Y6 obtained higher *P*(*E*,*T*) values of 76.3 and 76.7%, respectively, suggesting that the introduction of trialkylsilyl and Cl atom substitutions onto the SM-donors can improve the exciton dissociation and charge extraction of the devices, which is consistent with their higher FF values in devices. Moreover, to probe the effects of trialkylsilyl and Cl atom substitutions of SM-donors on the

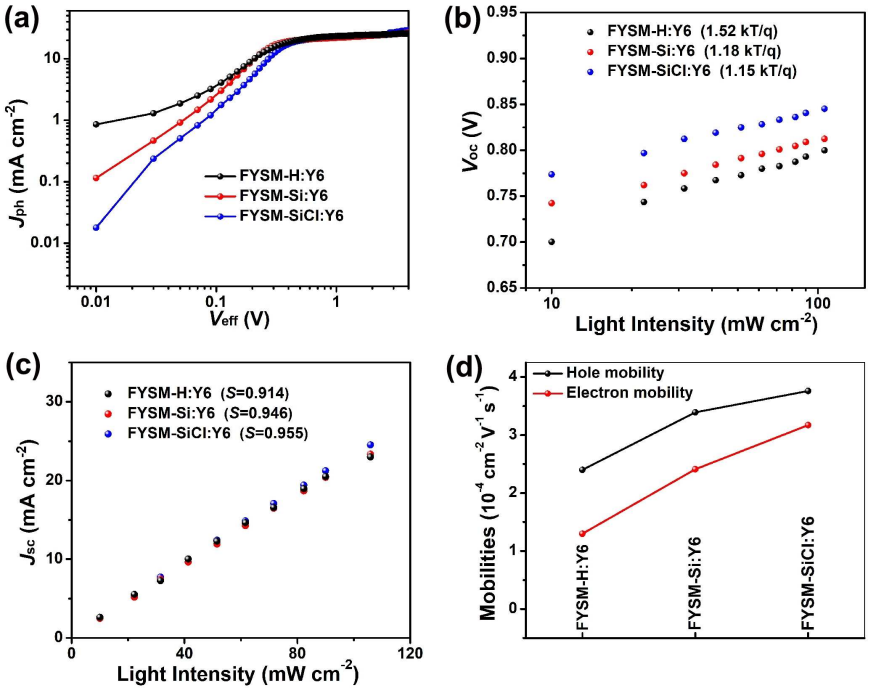

Figure 4. Curves of (a) J_{ph} vs. V_{eff}, (b) V_{oc} vs. light intensity, and (c) J_{sc} vs. light intensity measured from the Y6-based all-SM OSCs with different SM-donors. (d) μ_h and μ_e values of the Y6-based devices with different SM-donors measured by SCLC method.

charge recombination mechanisms of the devices, the dependence of V_{oc} and J_{sc} on light intensity (P) were studied.[23] As shown in Figure 4b of the plots of V_{oc} versus ln$P$, the devices based on FYSM–Si:Y6 and FYSM–SiCl:Y6 display similar slopes of 1.15–1.18 k_BT/q (where k_B, T, and q are the Boltzmann constant, Kelvin temperature, and elementary charge, respectively), which are close to 1.0 k_BT/q and much smaller than 1.52 k_BT/q from the FYSM–H:Y6-based device, suggesting less trap-assisted recombination after side-chain engineering of the SM-donors. In principle, the relationship of J_{sc} versus P is defined as $J_{sc} \propto P^S$.[23] As shown in the J_{sc} versus P plots in Figure 4c, the S value of the device based on FYSM–SiCl:Y6 was estimated as 0.955, which is closer to 1 and higher than the values from the devices based on FYSM–H:Y6 (0.914) and FYSM–Si:Y6 (0.946), indicating a reduced bimolecular recombination. Charge transport properties of the all-SM OSCs were also investigated by SCLC method. As displayed in Figure 4d, Figure S4, and Table S1, the FYSM–SiCl:Y6 blend also shows higher μ_h and electron-mobility (μ_e) of 3.76×10^{-4} and 3.17×10^{-4} cm^2 V^{-1} s^{-1} with a smaller μ_h/μ_e ratio of 1.19 compared to the blend films of FYSM–H:Y6 (2.20×10^{-4} and 1.30×10^{-4} cm^2 V^{-1} s^{-1}, $\mu_h/\mu_e = 1.85$) and FYSM–Si:Y6 (3.39×10^{-4} and 2.41×10^{-4} cm^2 V^{-1} s^{-1}, $\mu_h/\mu_e =$ 1.41), which helps to reduce accumulation of space charge in the all-SM OSCs. The more efficient exciton dissociation and charge extraction, less trap-assisted and bimolecular recombination, and reduced accumulation of space charge are conducive to the improved J_{sc} and FF values, thus achieving a higher PCE in the FYSM–SiCl:Y6-based devices.

Crystallinity and molecular packing properties of active layers were studied by GIWAXS measurements. As shown in Figure 5a of the 2D GIWAXS diffraction profiles, the FYSM–H:Y6 film shows a mixed orientation of "face-on" and "edge-on" with a slightly more "face-on" orientation. On the other hand, the FYSM–Si:Y6 and FYSM–SiCl:Y6 films present a "face-on" dominant orientation as indicated by the strong and dominant π–π stacking in the OOP direction. As shown in Figure 5b of the line-cuts from 2D patterns, among the three blend films, the FYSM–SiCl:Y6 film shows a more intense and sharper (010) diffraction peak in the OOP direction, suggesting a stronger intermolecular π–π stacking. Compared to the FYSM–H:Y6 film, the FYSM–Si:Y6 film shows a diffused (100) peak in the IP direction, while the FYSM–SiCl:Y6 film has a very sharp additional (100) peak at 3.49 nm^{-1} with a very high crystal coherence length (CCL) of 16.15 nm in the IP direction, which is consistent with the results of DSC measurements from SM-donor neat films. In the OOP direction, all the three blend films have similar π–π stacking distances of 0.35–0.36 nm but different CCL values. For the (010) peaks, compared to the FYSM–H:Y6 blend with a CCL value of 2.73 nm, the FYSM–Si:Y6 blend shows a slightly decreased CCL value of 2.51 nm, while the FYSM–SiCl:Y6 blend has a slightly higher CCL value of 2.96 nm. The difference in surface morphologies of active layers was probed via atomic force microscope (AFM) measurements. As shown in Figure 5c of the height images, with the introduction of trialkylsilyl and Cl atom substitutions onto SM-donors, the related active layers exhibit gradually increased root mean square roughness (R_q) values from FYSM–H:Y6 (1.98 nm) to FYSM–Si:Y6 (2.50 nm) and then to FYSM–SiCl:Y6 (4.90 nm). The significantly increased R_q value of FYSM–SiCl:Y6 is mainly due to the higher crystallinity and intermolecular interaction of FYSM–SiCl in blend film (see Figure 2a and Figure 5a,b). The FYSM–SiCl:Y6 blend with favourable molecular orientation and crystallinity is expected to restrain the trap-assisted recombination and enhance the charge transport in devices, and thus leading to higher J_{sc} and FF values.

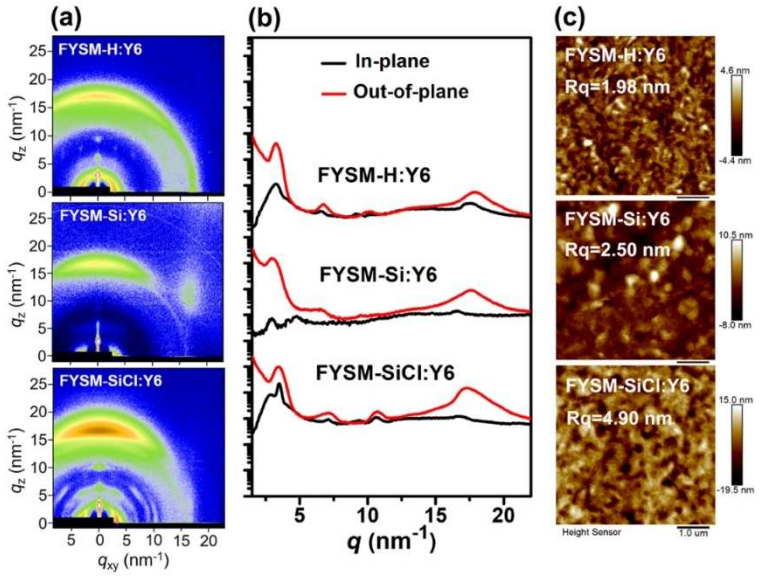

Figure 5. (a) GIWAXS images of the blend films and (b) corresponding line-cuts along the IP and OOP directions. (c) AFM images of the blend films.

Conclusion

Two novel small-molecule (SM)-donors, namely FYSM–Si and FYSM–SiCl, were developed by attaching the trialkylsilyl substitution, and both trialkylsilyl and Cl atom substitutions, respectively. From the original FYSM–H (2,6-(5′′-yl-3′,3′′-dihexyl-[2,2′:5′,2′′-terthiophene]-5-(3-hexyl-5-methylene-2-thioxothiazolidin-4-one))-4,8-bis(5-(2-ethylhexyl)thiophen-2-yl)benzo[1,2-*b*:4,5-*b*′]dithiophene) to FYSM–Si, and then FYSM–SiCl, the SM-donors show gradually deep-shifted HOMO levels and increased hole mobilities. Unlike the FYSM–H film with a predominantly "edge-on" orientation, the FYSM–SiCl film shows a primarily "face-on" orientation. Moreover, the introduction of both trialkylsilyl and Cl atom substitutions onto the SM-donors leads to improved molecular crystallinity and packing, and thus optimized blend film morphologies. As a result, compared to the FYSM–H-based all-SM OSCs with a power conversion efficiency (PCE) of 10.9%, the FYSM–SiCl-based ones achieved a much high PCE of 13.4% benefitted from both higher open-circuit voltage (V_{oc} = 0.85 V) and short-circuit current density (J_{sc} = 23.7 mA cm^{-2}), while the FYSM–Si-based ones attained a moderate PCE of 12.2%. This work offers a promising method to design efficient SM-donors by side-chain engineering strategy via the introduction of both trialkylsilyl and Cl atom substitutions.

Experimental Section

Synthesis method: Compounds BDT-T-Sn, BDT-TSi-Sn, and BDT-TSiCl-Sn were synthesized according to the references.[22a,25] Compound 3 and SM-acceptor Y6 were purchased from 1-Material Inc. and Solarmer Materials Inc., respectively. SM-donors FYSM–H, FYSM–Si, and FYSM–SiCl were synthesized according to following procedures:

BDT-T-3T-CHO: In a dry 50 mL flask, $Pd(PPh_3)_4$ (25 mg) was added to a solution of BDT-T-Sn (150 mg, 0.166 mmol) and 3 (200 mg, 0.382 mmol) in 15 mL degassed toluene under argon and stirred vigorously at 110 °C for 24 h. After the system cooled to room temperature, it was quenched with saturated aqueous solution of sodium acetate and extracted with CH_2Cl_2. The combined extracts were washed with brine, dried over anhydrous $MgSO_4$, and then filtered and collected in solvent. The solvent was removed by rotary evaporation to yield the crude product, which was then purified by column chromatography on silica gel with hexane/CH_2Cl_2 (*v*/*v* = 2:1) as eluent to afford BDT-T-3T-CHO as a red solid (110 mg, 45%). ^{1}H NMR (400 MHz, $CDCl_3$, TMS), (ppm): δ = 9.89 (s, 2H), 7.71 (d, *J* = 4.0 Hz, 2H), 7.63 (s, 2H), 7.31 (d, *J* = 3.5 Hz, 2H), 7.23 (d, *J* = 4.0 Hz, 2H), 7.12 (s, 2H), 7.01 (s, 2H), 6.94 (d, *J* = 3.5 Hz, 2H), 2.90 (dd, *J* = 6.7, 3.5 Hz, 4H), 2.80 (ddd, *J* = 20.7, 13.1, 5.4 Hz, 8H), 1.68 (dq, *J* = 7.9, 5.5 Hz, 10H), 1.51–1.22 (m, 40H), 1.02–0.85 (m, 24H).

BDT-TSi-3T-CHO: In a dry 50 mL flask, $Pd(PPh_3)_4$ (25 mg) was added to a solution of compounds BDT-TSi-Sn (173 mg, 0.174 mmol) and 3 (210 mg, 0.401 mmol) in 15 mL degassed toluene under argon and stirred vigorously at 110 °C for 24 h. After the system cooled to room temperature, it was quenched with saturated aqueous solution of sodium acetate and extracted with CH_2Cl_2. The combined extracts were washed with brine, dried over anhydrous $MgSO_4$, and then filtered and collected in solvent. The solvent was removed by rotary evaporation to yield the crude product, which was then purified by column chromatography on silica gel with hexane/CH_2Cl_2 (*v*/*v* = 2:1) as eluent to afford BDT-TSi-3T-CHO as a red solid (170 mg, 63%). ^{1}H NMR (400 MHz, $CDCl_3$, TMS), (ppm): δ = 9.89 (s, 2H), 7.71 (d, *J* = 4.0 Hz, 2H), 7.63 (s, 2H), 7.59 (d, *J* = 3.4 Hz, 2H), 7.40 (d, *J* = 3.4 Hz, 2H), 7.23 (d, *J* = 4.0 Hz, 2H), 7.12 (s, 2H), 7.01 (s, 2H), 2.80 (ddd, *J* = 20.5, 14.0, 6.3 Hz, 8H), 1.74–1.62 (m, 8H), 1.44 (tt, *J* = 11.8, 6.0 Hz, 28H), 1.32 (dd, *J* = 7.3, 3.3 Hz, 20H), 0.99–0.86 (m, 30H).

BDT-TSiCl-3T-CHO: In a dry 50 mL flask, $Pd(PPh_3)_4$ (25 mg) was added to a solution of compounds BDT-TSiCl-Sn (230 mg, 0.216 mmol) and 3 (260 mg, 0.50 mmol) in 15 mL degassed toluene under argon and stirred vigorously at 110 °C for 24 h. After the system cooled to room temperature, it was quenched with saturated aqueous solution of sodium acetate and extracted with CH_2Cl_2. The combined extracts were washed with brine, dried over anhydrous $MgSO_4$, and then filtered and collected in solvent. The solvent was removed by rotary evaporation to yield the crude product, which was then purified by column chromatography on silica gel with hexane/CH_2Cl_2 (*v*/*v* = 2:1) as eluent to afford BDT-TSiCl-3T-CHO as a red solid (190 mg, 54%). ^{1}H NMR (400 MHz, $CDCl_3$, TMS), (ppm): δ = 9.89 (s, 2H), 7.72 (d, *J* = 4.0 Hz, 2H), 7.56 (s, 2H), 7.42 (s, 2H), 7.24 (d, *J* = 4.0 Hz, 2H), 7.15 (s, 2H), 7.04 (s, 2H), 2.86–2.73 (m, 8H), 1.78–1.63 (m, 8H), 1.51 (ddd, *J* = 11.2, 5.7, 3.4 Hz, 12H), 1.47–1.38 (m, 8H), 1.33 (td, *J* = 6.7, 3.8 Hz, 16H), 1.09–0.97 (m, 30H), 0.90 (t, *J* = 7.0 Hz, 12H).

FYSM–H: In a dry 50 mL flask, compounds BDT-T-3T-CHO (90 mg, 0.0615 mmol), 4 (80 g, 0.369 mmol), and piperidine (0.25 mL) were added to 10 mL of degassed chloroform under argon and stirred vigorously at 65 °C for 12 h. Then the mixture was poured into methanol (100 mL) followed by precipitation, and the sediments were collected. The resulting crude compound was purified by column chromatography on silica gel with hexane/CH_2Cl_2 (*v*/*v* = 2:1) as eluent and then was recrystallized two times by a mixed solvent of chloroform/acetone to give FYSM–H as a red solid (50 mg, 44%). ^{1}H NMR (400 MHz, $CDCl_3$, TMS), (ppm): δ = 7.82 (s, 2H), 7.59 (s, 2H), 7.34 (d, *J* = 3.4 Hz, 4H), 7.19 (d, *J* = 4.0 Hz, 2H), 7.09 (s, 2H), 6.99 (s, 2H), 6.97 (d, *J* = 3.5 Hz, 2H), 4.16–4.05 (m, 4H), 2.94 (dd, *J* = 6.7, 2.4 Hz, 4H), 2.86–2.69 (m, 8H), 1.72 (dt, *J* = 15.4, 7.5 Hz, 14H), 1.55–1.29 (m, 52H), 1.09–0.87 (m, 30H). ^{13}C NMR (150 MHz, $CDCl_3$, TMS), (ppm): δ = 192.15, 167.48, 145.99, 144.30, 141.89, 140.95, 138.64, 137.36, 137.31, 137.00, 136.83, 135.65, 135.41, 130.51, 129.69, 128.96, 128.34, 127.86, 126.43, 125.49, 124.95, 123.28, 120.15, 119.12, 44.86, 41.52, 31.73, 31.69, 31.34, 29.35, 23.11, 22.69, 22.65, 22.52, 14.26, 14.15, 14.02, 11.02. MALDI-TOF MS (*m*/*z*) for $C_{102}H_{128}N_2O_2S_{14}$, Calcd: 1863.03, Found: 1862.92.

FYSM–Si: In a dry 50 mL flask, compounds BDT-TSi-3T-CHO (250 mg, 0.161 mmol), 4 (210 g, 0.966 mmol), and piperidine (0.5 mL) were added to 20 mL of degassed chloroform under argon and stirred vigorously at 65 °C for 12 h. Then the mixture was poured into methanol (100 mL) followed by precipitation, and the sediments were collected. The resulting crude compound was purified by column chromatography on silica gel with hexane/CH_2Cl_2 (*v*/*v* = 2:1) as eluent and then was recrystallized two times by a mixed solvent of chloroform/acetone to give FYSM–Si as a red solid (105 mg, 33%). ^{1}H NMR (400 MHz, $CDCl_3$, TMS), (ppm): δ = 7.82 (s, 2H), 7.61–7.57 (m, 4H), 7.41 (d, *J* = 3.4 Hz, 2H), 7.34 (d, *J* = 4.2 Hz, 2H), 7.18 (d, *J* = 4.0 Hz, 2H), 7.08 (s, 2H), 6.98 (s, 2H), 4.12–4.05 (m, 4H), 2.78 (dt, *J* = 18.7, 7.2 Hz, 8H), 1.75–1.61 (m, 12H), 1.52–1.39 (m, 30H), 1.39–1.27 (m, 30H), 0.93 (ddd, *J* = 11.1, 10.6, 6.4 Hz, 36H). ^{13}C NMR (150 MHz, $CDCl_3$, TMS), (ppm): δ = 192.19, 167.51, 144.48, 144.28, 141.92, 141.02, 139.50, 138.58, 137.52, 137.29, 137.07, 135.63, 135.40, 134.98, 134.58, 129.70, 129.12, 129.02, 126.50, 124.97, 123.26, 120.22, 119.13, 44.88, 31.71, 31.35, 29.33, 28.74, 28.48, 28.15, 22.67, 22.63, 22.52, 14.14, 14.02, 13.93, 13.27.

FYSM–SiCl: In a dry 50 mL flask, compounds BDT-TSiCl-3T-CHO (170 g, 0.105 mmol), 4 (140 g, 0.629 mmol), and piperidine (0.5 mL) were added to 20 mL of degassed chloroform under argon and stirred vigorously at 65 °C for 12 h. Then the mixture was poured into methanol (100 mL) followed by precipitation, and the sediments were collected. The resulting crude compound was purified by column chromatography on silica gel with hexane/CH_2Cl_2 (v/v = 2:1) as eluent and then was recrystallized two times by a mixed solvent of chloroform/acetone to give FYSM–SiCl as a red solid (83 mg, 39%). ^{1}H NMR (400 MHz, $CDCl_3$, TMS), (ppm): δ = 7.82 (s, 2H), 7.54 (s, 2H), 7.44 (s, 2H), 7.34 (d, J = 3.8 Hz, 2H), 7.20 (d, J = 3.9 Hz, 2H), 7.12 (s, 2H), 7.01 (s, 2H), 4.09 (t, J = 7.5 Hz, 4H), 2.87–2.74 (m, 8H), 1.77–1.66 (m, 12H), 1.56–1.43 (m, 16H), 1.42–1.26 (m, 32H), 1.15–1.00 (m, 30H), 0.93 (dt, J = 13.6, 5.4 Hz, 18H). ^{13}C NMR (150 MHz, $CDCl_3$, TMS), (ppm): δ = 192.13, 167.47, 144.16, 143.89, 141.90, 141.05, 138.48, 138.07, 137.18, 137.10, 135.41, 134.93, 134.58, 132.24, 131.98, 131.00, 130.19, 129.86, 129.13, 128.75, 128.51, 124.91, 122.33, 120.24, 118.53, 44.85, 31.71, 31.67, 31.34, 29.71, 29.34, 29.31, 28.46, 22.67, 22.64, 22.52, 18.51, 17.54, 15.64, 14.15, 14.02. MALDI-TOF MS (m/z) for $C_{104}H_{134}Cl_2N_2O_2S_{14}Si_2$, Calcd: 2020.18, Found: 2020.56.

Acknowledgements

We thank the Swedish Research Council (2015-04853, 2016-06146, and 2019-04683), the Swedish Research Council Formas, the Knut and Alice Wallenberg Foundation (2017.0186 and 2016.0059) and the Open Fund of the State Key Laboratory of Luminescent Materials and Devices (South China University of Technology, 2020-skllmd-07) for financial support. W.S. thanks the project funded by China Postdoctoral Science Foundation (2020M673054), Postdoctoral Fund of Jinan University, and National Natural Science Foundation of China (22005121). L.H. thanks the NSFC Project (61774077), Key Projects of Joint Fund of Basic and Applied Basic Research Fund of Guangdong Province (2019B1515120073, 2019B090921002), Guangdong Science and Technology Research Foundation (2020A1414010036) and Guangzhou Key laboratory of Vacuum Coating Technologies and New Energy Materials Open Projects Fund (KFVE20200006) for financial support. Y.L. thanks the financial support from the Science and Technology Program of Shanxi Province (2019JQ-244). M.Z. and X.G. acknowledges financial support from National Natural Science Foundation of China (NSFC) (No. 51773142 and 51973146), the Jiangsu Provincial Natural Science Foundation (Grant No. BK20190099), Collaborative Innovation Center of Suzhou Nano Science & Technology, the Priority Academic Program Development of Jiangsu Higher Education Institutions.

Conflict of Interest

The authors declare no conflict of interest.

Keywords: crystalline donor · organic solar cells · photovoltaics · power conversion efficiency · side chain engineering

[1] Y. Li, *Acc. Chem. Res.* **2012**, *45*, 723.
[2] C. Yan, S. Barlow, Z. Wang, H. Yan, A. K.-Y. Jen, S. R. Marder, X. Zhan, *Nat. Rev. Mater.* **2018**, *3*, 18003.
[3] a) Q. Fan, W. Su, S. Chen, W. Kim, X. Chen, B. Lee, T. Liu, U. A. Mendez-Romero, R. Ma, T. Yang, W. Zhuang, Y. Li, Y. Li, T. Kim, L. Hou, C. Yang, H. Yan, D. Yu, E. Wang, *Joule* **2020**, *4*, 658; b) H. Fu, Y. Li, J. Yu, Z. Wu, Q. Fan, F. Lin, H. Y. Woo, F. Gao, Z. Zhu, A. K.-Y. Jen, *J. Am. Chem. Soc.* **2021**, *143*, 2665; c) Q. Fan, W. Su, S. Chen, T. Liu, W. Zhuang, R. Ma, X. Wen, Z. Yin, Z. Luo, X. Guo, L. Hou, K. Moth-Poulsen, Y. Li, Z. Zhang, C. Yang, D. Yu, H. Yan, M. Zhang, E. Wang, *Angew. Chem. Int. Ed.* **2020**, *59*, 19835; *Angew. Chem.* **2020**, *132*, 20007.
[4] Y. Lin, J. Wang, Z. Zhang, H. Bai, Y. Li, D. Zhu, X. Zhan, *Adv. Mater.* **2015**, *27*, 1170.
[5] J. Yuan, Y. Zhang, L. Zhou, G. Zhang, H.-L. Yip, T.-K. Lau, X. Lu, C. Zhu, H. Peng, P. A. Johnson, M. Leclerc, Y. Cao, J. Ulanski, Y. Li, Y. Zou, *Joule* **2019**, *3*, 1140.
[6] a) C. Zhu, J. Yuan, F. Cai, L. Meng, H. Zhang, H. Chen, J. Li, B. Qiu, H. Peng, S. Chen, Y. Hu, C. Yang, F. Gao, Y. Zou, Y. Li, *Energy Environ. Sci.* **2020**, *13*, 2459; b) M. Zhang, L. Zhu, G. Zhou, T. Hao, C. Qiu, Z. Zhao, Q. Hu, B. W. Larson, H. Zhu, Z. Ma, Z. Tang, W. Feng, Y. Zhang, T. P. Russell, F. Liu, *Nat. Commun.* **2021**, *12*, 309; c) Q. An, J. Wang, X. Ma, J. Gao, Z. Hu, B. Liu, H. sun, X. Guo, X. L. Zhang, F. Zhang, *Energy Environ. Sci.* **2020**, *13*, 5039; d) L. Meng, Y. Zhang, X. Wan, C. Li, X. Zhang, Y. Wang, X. Ke, Z. Xiao, L. Ding, R. Xia, H. Yip, Y. Cao, Y. Chen, *Science* **2018**, *361*, 1094.
[7] a) J. Yao, B. Qiu, Z.-G. Zhang, L. Xue, R. Wang, C. Zhang, S. Chen, Q. Zhou, C. Sun, C. Yang, M. Xiao, L. Meng, Y. Li, *Nat. Commun.* **2020**, *11*, 2726; b) Y. Lin, M. I. Nugraha, Y. Firdaus, A. D. Scaccabarozzi, F. Anies, A.-H. Emwas, E. Yengel, X. Zheng, J. Liu, W. Wahyudi, E. Yarali, H. Faber, O. M. Bakr, L. Tsetseris, M. Heeney, T. D. Anthopoulos, *ACS Energy Lett.* **2020**, *5*, 3663; c) R. Ma, T. Liu, Z. Luo, K. Gao, K. Chen, G. Zhang, W. Gao, Y. Xiao, T.-K. Lau, Q. Fan, Y. Chen, L.-K. Ma, H. Sun, G. Cai, T. Yang, X. Lu, E. Wang, C. Yang, A. K.-Y. Jen, H. Yan, *ACS Energy Lett.* **2020**, *5*, 2711; d) L. Ye, Y. Cai, C. Li, L. Zhu, J. Xu, K. Weng, K. Zhang, M. Huang, M. Zeng, T. Li, E. Zhou, S. Tan, X. Hao, Y. Yi, F. Liu, Z. Wang, X. Zhan, Y. Sun, *Energy Environ. Sci.* **2020**, *13*, 5117.
[8] a) X. Guo, Q. Fan, J. Wu, G. Li, Z. Peng, W. Su, J. Lin, L. Hou, Y. Qin, H. Ade, L. Ye, M. Zhang, Y. Li, *Angew. Chem. Int. Ed.* **2021**, *60*, 2322; *Angew. Chem.* **2021**, *133*, 2352; b) H. Chen, H. Lai, Z. Chen, Y. Zhu, H. Wang, L. Han, Y. Zhang, F. He, *Angew. Chem. Int. Ed.* **2021**, *60*, 3238; *Angew. Chem.* **2021**, *133*, 3275; c) T. Wang, R. Sun, M. Shi, F. Pan, Z. Hu, F. Huang, Y. Li, J. Min, *Adv. Energy Mater.* **2020**, *10*, 2000590; d) Q. Liu, Y. Jiang, K. Jin, J. Qin, J. Xu, W. Li, J. Xiong, J. Liu, Z. Xiao, K. Sun, S. Yang, X. Zhang, L. Ding, *Sci. Bull.* **2020**, *65*, 272.
[9] a) F. Lin, K. Jiang, W. Kaminsky, Z. Zhu, A. K.-Y. Jen, *J. Am. Chem. Soc.* **2020**, *142*, 15246; b) W. Gao, H. Fu, Y. Li, F. Lin, R. Sun, Z. Wu, X. Wu, C. Zhong, J. Min, J. Luo, H. Y. Woo, Z. Zhu, A. K.-Y. Jen, *Adv. Energy Mater.* **2021**, *11*, 2003177; c) Y. Cui, H. Yao, J. Zhang, K. Xian, T. Zhang, L. Hong, Y. Wang, Y. Xu, K. Ma, C. An, C. He, Z. Wei, F. Gao, J. Hou, *Adv. Mater.* **2020**, *32*, 1908205.
[10] a) H. Fu, W. Gao, Y. Li, F. Lin, X. Wu, J. H. Son, J. Luo, H. Y. Woo, Z. Zhu, A. K.-Y. Jen, *Small Methods* **2020**, *4*, 2000687; b) L. Zhan, S. Li, X. Xia, Y. Li, X. Lu, L. Zuo, M. Shi, H. Chen, *Adv. Mater.* **2021**, *33*, 2007231; c) Y. Wei, J. Yu, L. Qin, H. Chen, X. Wu, Z. Wei, X. Zhang, L. Ding, F. Gao, H. Huang, *Energy Environ. Sci.* **2021**, *14*, 2314.
[11] a) H. Tang, C. Yan, J. Huang, Z. Kan, Z. Xiao, K. Sun, G. Li, S. Lu, *Matter* **2020**, *3*, 1403; b) B. Kan, Y. Kan, L. Zuo, X. Shi, K. Gao, *InfoMat* **2021**, *3*, 175; c) X. Wan, C. Li, M. Zhang, Y. Chen, *Chem. Soc. Rev.* **2020**, *49*, 2828; d) Y. Huo, H.-L. Zhang, X. Zhan, *ACS Energy Lett.* **2019**, *4*, 1241; e) J.-L. Wang, K.-K. Liu, J. Yan, Z. Wu, F. Liu, F. Xiao, Z.-F. Chang, H.-B. Wu, Y. Cao, T. P. Russell, *J. Am. Chem. Soc.* **2016**, *138*, 7687.
[12] a) L. Nian, Y. Kan, K. Gao, M. Zhang, N. Li, G. Zhou, S. B. Jo, X. Shi, F. Lin, Q. Rong, F. Liu, G. Zhou, A. K.-Y. Jen, *Joule* **2020**, *4*, 2223; b) K. Gao, S. B. Jo, X. Shi, L. Nian, M. Zhang, Y. Kan, F. Lin, B. Kan, B. Xu, Q. Rong, L. Shui, F. Liu, X. Peng, G. Zhou, Y. Cao, A. K.-Y. Jen, *Adv. Mater.* **2019**, *31*, 1807842; c) K. Sun, Z. Xiao, S. Lu, W. Zajaczkowski, W. Pisula, E. Hanssen, J. M. White, R. M. Williamson, J. Subbiah, J. Ouyang, A. B. Holmes, W. W. H. Wong, D. J. Jones, *Nat. Commun.* **2015**, *6*, 6013; d) Q. Fan, T. Liu, M. Zhang, W. Su, U. A. Méndez-Romero, T. Yang, X. Geng, L. Hou, D. Yu, F. Liu, H. Yan, E. Wang, *Small Methods* **2020**, *4*, 1900766; e) J.-L. Wang, K.-K. Liu, S. Liu, F. Xiao, Z.-F. Chang, Y.-Q. Zheng, J.-H. Dou, R.-B. Zhang, H.-B. Wu, J. Pei, Y. Cao, *Chem. Mater.* **2017**, *29*, 1036.
[13] a) R.-Z. Liang, Y. Zhang, V. Savikhin, M. Babics, Z. Kan, M. Wohlfahrt, N. Wehbe, S. Liu, T. Duan, M. F. Toney, F. Laquai, P. M. Beaujuge, *Adv. Energy Mater.* **2019**, *9*, 1802836; b) Q. Zhang, B. Kan, F. Liu, G. Long, X.

Wan, X. Chen, Y. Zuo, W. Ni, H. Zhang, M. Li, Z. Hu, F. Huang, Y. Cao, Z. Liang, M. Zhang, T. P. Russell, Y. Chen, *Nat. Photonics* **2015**, *9*, 35; c) J. Wan, X. Xu, G. Zhang, Y. Li, K. Feng, Q. Peng, *Energy Environ. Sci.* **2017**, *10*, 1739.

[14] R. Zhou, Z. Jiang, C. Yang, J. Yu, J. Feng, M. A. Adil, D. Deng, W. Zou, J. Zhang, K. Lu, W. Ma, F. Gao, Z. Wei, *Nat. Commun.* **2019**, *10*, 5393.

[15] R. Sun, Y. Wu, J. Guo, Z. Luo, C. Yang, J. Min, *Sci. China Chem.* **2020**, *63*, 1246.

[16] a) H. Tang, T. Xu, C. Yan, J. Gao, H. Yin, J. Lv, R. Singh, M. Kumar, T. Duan, Z. Kan, S. Lu, G. Li, *Adv. Sci.* **2019**, *6*, 1901613; b) L. Yang, S. Zhang, C. He, J. Zhang, Y. Yang, J. Zhu, Y. Cui, W. Zhao, H. Zhang, Y. Zhang, Z. Wei, J. Hou, *Chem. Mater.* **2018**, *30*, 2129; c) X. Li, Y. Wang, Q. Zhu, X. Guo, W. Ma, X. Ou, M. Zhang, Y. Li, *J. Mater. Chem. A* **2019**, *7*, 3682.

[17] a) Y. Huo, X.-T. Gong, T.-K. Lau, T. Xiao, C. Yan, X. Lu, G. Lu, X. Zhan, H.-L. Zhang, *Chem. Mater.* **2018**, *30*, 8661; b) Y. Wang, Y. Wang, L. Zhu, H. Liu, J. Fang, X. Guo, F. Liu, Z. Tang, M. Zhang, Y. Li, *Energy Environ. Sci.* **2020**, *13*, 1309; c) J. Fang, C. Ye, X. Wang, Y. Wang, X. Guo, Q. Fan, W. Ma, M. Zhang, *Org. Electron.* **2019**, *67*, 175; d) H. Bin, Y. Yang, Z.-G. Zhang, L. Ye, M. Ghasemi, S. Chen, Y. Zhang, C. Zhang, C. Sun, L. Xue, C. Yang, H. Ade, Y. Li, *J. Am. Chem. Soc.* **2017**, *139*, 5085.

[18] a) H. Chen, D. Hu, Q. Yang, J. Gao, J. Fu, K. Yang, H. He, S. Chen, Z. Kan, T. Duan, C. Yang, J. Ouyang, Z. Xiao K Sun, S. Lu, *Joule* **2019**, *3*, 3034; b) H. Tang, H. Chen, C. Yan, J. Huang, P. W. K. Fong, J. Lv, D. Hu, R. Singh, M. Kumar, Z. Xiao, Z. Kan, S. Lu, G. Li, *Adv. Energy Mater.* **2020**, *10*, 2001076.

[19] a) B. Qiu, Z. Chen, S. Qin, J. Yao, W. Huang, L. Meng, H. Zhu, Y. Yang, Z.-G. Zhang, Y. Li, *Adv. Mater.* **2020**, *32*, 1908373; b) J. Ge, L. Xie, R. Peng, B. Fanady, J. Huang, W. Song, T. Yan, W. Zhang, Z. Ge, *Angew. Chem. Int. Ed.* **2020**, *59*, 2808; *Angew. Chem.* **2020**, *132*, 2830; c) Q. Yue, H. Wu, Z. Zhou, M. Zhang, F. Liu, X. Zhu, *Adv. Mater.* **2019**, *31*, 1904283.

[20] H. Bin, J. Wang, J. Li, M. M. Wienk, R. A. J. Janssen, *Adv. Mater.* **2021**, *33*, 2008429.

[21] a) J. Qin, C. An, J. Zhang, K. Ma, Y. Yang, T. Zhang, S. Li, K. Xian, Y. Cui, Y. Tang, W. Ma, H. Yao, S. Zhang, B. Xu, C. He, J. Hou, *Sci. China Mater.* **2020**, *63*, 1142; b) H. Bin, J. Yao, Y. Yang, l. Angunawela, C. Sun, L. Gao, L. Ye, B. Qiu, L. Xue, C. Zhu, C. Yang, Z.-G. Zhang, H. Ade, Y. Li, *Adv. Mater.* **2018**, *30*, 1706361.

[22] a) W. Su, G. Li, Q. Fan, Q. Zhu, X. Guo, J. Chen, J. Wu, W. Ma, M. Zhang, Y. Li, *J. Mater. Chem. A* **2019**, *7*, 2351; b) Q. Fan, Q. Zhu, Z. Xu, W. Su, J. Chen, J. Wu, X. Guo, W. Ma, M. Zhang, Y. Li, *Nano Energy* **2018**, *48*, 413.

[23] a) C. Xu, J. Wang, Q. An, X. Ma, Z. Hu, J. Gao, J. Zhang, F. Zhang, *Nano Energy* **2019**, *66*, 104119; b) Q. Fan, R. Ma, T. Liu, J. Yu, Y. Xiao, W. Su, G. Cai, Y. Li, W. Peng, T. Guo, Z. Luo, H. Sun, L. Hou, W. Zhu, X. Lu, D. Yu, F. Gao, E. Moons, H. Yan, E. Wang, *Sci. China Chem.* **2021**, DOI: 10.1007/s11426-021-1020-7; c) Z. Zhou, S. Xu, J. Song, Y. Jin, Q. Yue, Y. Qian, F. Liu, F. Zhang, X. Zhu, *Nat. Energy* **2018**, *3*, 952.

[24] a) Q. Fan, H. Fu, Q. Wu, Z. Wu, F. Lin, Z. Zhu, J. Min, H. Y. Woo, A. K.-Y. Jen, *Angew. Chem. Int. Ed.* **2021**, DOI: 10.1002/anie.202101577; *Angew. Chem.* **2021**, DOI: 10.1002/ange.202101577; b) Q. Fan, Q. An, Y. Lin, Y. Xia, Q. Li, M. Zhang, W. Su, W. Peng, C. Zhang, F. Liu, L. Hou, W. Zhu, D. Yu, M. Xiao, E. Moons, F. Zhang, T. D. Anthopoulos, O. Inganäs, E. Wang, *Energy Environ. Sci.* **2020**, *13*, 5017.

[25] H. Bin, L. Gao, Z.-G. Zhang, Y. Yang, Y. Zhang, C. Zhang, S. Chen, L. Xue, C. Yang, M. Xiao, Y. Li, *Nat. Commun.* **2016**, *7*, 13651.

Manuscript received: April 16, 2021
Revised manuscript received: May 27, 2021
Accepted manuscript online: May 31, 2021
Version of record online: ■■, ■■■

FULL PAPERS

Superb substitution: A small molecule donor FYSM–SiCl with trialkylsilyl and chlorine substitutions is developed. Compared to its unsubstituted analogue FYSM–H, FYSM–SiCl has a deep-shifted highest occupied molecular orbital level, improved crystallinity and hole-mobility, and a predominantly "face-on" orientation. FYSM–SiCl-based all-small-molecule solar cells achieve a much higher power conversion efficiency of 13.4% compared to the FYSM–H-based ones (10.9%).

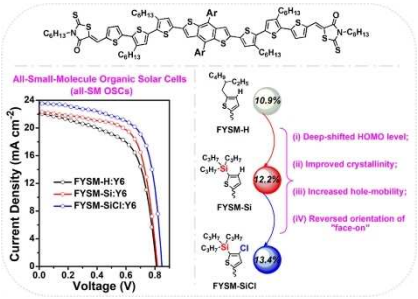

Dr. W. Su, Y. Wang, Z. Yin, Dr. Q. Fan, Prof. X. Guo, Dr. L. Yu*, Dr. Y. Li, Prof. L. Hou*, Prof. M. Zhang*, Prof. Q. Peng, Prof. Y. Li, Prof. E. Wang**